



Cite this: *Chem. Commun.*, 2015,
51, 10925

Received 24th April 2015,
Accepted 22nd May 2015

DOI: 10.1039/c5cc03398e

www.rsc.org/chemcomm

Synthesis of nanocrystals of Zr-based metal–organic frameworks with csq-net: significant enhancement in the degradation of a nerve agent simulant†

Peng Li,^a Rachel C. Klet,^a Su-Young Moon,^a Timothy C. Wang,^a Pravas Deria,^a Aaron W. Peters,^a Benjamin M. Klahr,^a Hea-Jung Park,^a Salih S. Al-Juaid,^b Joseph T. Hupp^{*a} and Omar K. Farha^{*ab}

The synthesis of nano-sized particles of NU-1000 (length from 75 nm to 1200 nm) and PCN-222/MOF-545 (length from 350 nm to 900 nm) is reported. The catalytic hydrolysis of methyl paraoxon was investigated as a function of NU-1000 crystallite size and a significant enhancement in the rate was observed for the nano-sized crystals compared to microcrystals.

Metal–organic frameworks (MOFs)¹ have been widely evaluated for gas storage,² gas separation,³ sensing,⁴ and heterogeneous catalysis⁵ due to their exceptional tunability, high surface area and porosity.⁶ MOFs are known to catalyze many reactions using Lewis acidic sites on the nodes,⁷ or by incorporation of transition metals⁸ or functional groups on linkers⁹ and/or nodes.^{8a} However, most of the reported MOFs in the past decade have a microporous structure,¹⁰ which restricts molecular diffusion and transport through the material, and often limits catalysis to the surface sites of MOF crystallites. Recently, several MOFs featuring larger pores (mesopores) have been reported which can significantly reduce diffusion limitations.¹¹ Indeed, catalysis with these MOFs typically yields improved catalytic efficiencies compared to microporous MOFs, presumably due to catalysis occurring at both interior and exterior sites.¹²

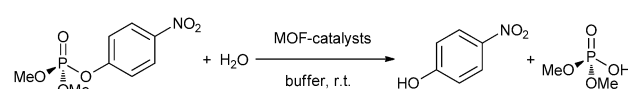
Nano-sized MOF particles, with larger relative external surface areas, have also been recently described.¹³ These nano-sized particles should not only give higher efficiencies for surface-only catalysis, but also promise to open up new applications for MOFs such as drug delivery,¹⁴ biomedical imaging,¹⁵ and biological assays.¹⁶ For these biomedical applications, customized nano-sized crystals are necessary for facile transport through capillary vessels or the lymphatic system, as well as for effective

cellular uptake. Combining nano-sized MOFs with the aforementioned advantages of mesoporous MOFs would potentially lead to a new generation of MOF materials for a wide variety of applications.

In the past decade, tremendous effort has been devoted to developing effective approaches to precisely control the crystallite size of MOFs in the nano regime. Several microporous MOFs, including HKUST-1,^{13d,f} MOF-5,^{13g} MOF-177,¹⁷ UiO-66,^{13b} ZIF-7,¹⁸ and ZIF-8,^{13e} have been synthesized as nanocrystals by various synthetic methods, including ultrasound and microwave synthesis,¹⁹ microemulsion synthesis,²⁰ surfactant mediated hydrothermal syntheses,²¹ and the coordination modulation method.^{13d} In addition, the synthesis of nano-sized mesoporous MOFs has also been reported,^{13h} indicating the feasibility of preparing nano-sized mesoporous MOFs.

Recently, zirconium-based MOFs have been extensively studied due to their high thermal, mechanical, and hydrolytic stabilities.^{11a,22} Our group has investigated the catalytic activity of several MOFs with Zr₆ nodes, namely, UiO-66, its derivatives, and NU-1000, for the degradation of nerve agents and/or their simulants (Scheme 1).²³ While UiO-66 and UiO-67 feature 12-connected Zr₆ nodes, NU-1000 presents 8-connected Zr₆ nodes and contains terminal water and hydroxyl ligands in addition to μ_3 -bridging hydroxyl and oxido groups. NU-1000 also has the advantage of wide mesoporous channels (31 Å) that allow for diffusion of the substrate throughout the material (and consequently catalysis at interior sites), which ultimately leads to superior catalytic activity.^{23a}

In order to further improve the catalytic activity of NU-1000, we sought to synthesize nano-sized particles of NU-1000, which should have larger relative external surface areas, and therefore



Scheme 1 Hydrolysis of methyl paraoxon using MOF-catalysts.

^a Department of Chemistry, Northwestern University, 2145 Sheridan Road, Evanston, Illinois 60208, USA. E-mail: o-farha@northwestern.edu,

j-hupp@northwestern.edu; Tel: +1-847-491-3504

^b Department of Chemistry, Faculty of Science, King Abdulaziz University, Jeddah, Saudi Arabia

† Electronic supplementary information (ESI) available: Experimental details, PXRD, TGA analysis, and DLS data. See DOI: 10.1039/c5cc03398e

faster rates of methyl paraoxon hydrolysis. Herein, we report the synthesis of NU-1000 nano-sized crystallites ranging in size from 75 nm up to 1200 nm (length) and their respective rates of hydrolysis for methyl paraoxon; 15 000 nm-sized NU-1000 particles were also synthesized based on previous literature methods and tested for hydrolysis for comparison.^{11a} In addition, the synthesis of nano-sized PCN-222/MOF-545,^{11b} a related mesoporous zirconium MOF with same csq-net to NU-1000, is also described.

Previous reports have relied primarily on the use of modulators (non-bridging ligands that compete with linkers for node coordination) to control nucleation and obtain crystallites in a desired size range, in addition to other factors contributing to crystal growth such as temperature and concentration.^{13b,d} Extension of these methods to Zr₆-based MOFs with tetratopic linkers is not straightforward since different nets can be formed including fcu, ftw, scu, and, of course, csq.²⁴ For example, the linker in NU-1000, 1,3,6,8-tetrakis(*p*-benzoic acid)pyrene, with a Zr(IV) salt (ZrCl₄ or ZrOCl₂·8H₂O) can form either NU-1000 or NU-901.^{11a,25} Similarly, at least three distinct phases (PCN-221/MOF-525,^{11c,26} PCN-222/MOF-545,^{11b,c} and PCN-223²⁷) are accessible with the tetracarboxylate porphyrin linker used for PCN-222/MOF-545. As the realization of these phases is often very sensitive to the concentration of the modulator, it can be challenging to obtain the desired pure phase, in the desired crystallite size regime, solely by altering the modulator concentration. Accordingly, we found that for NU-1000 lowering the concentration of benzoic acid (BA)—the typical modulator used to promote formation of Zr₆ clusters to obtain the desired phase—while adding a secondary monocarboxylic acid modulator, trifluoroacetic acid (TFA), resulted in formation of nano-sized crystallites. Similarly, with PCN-222/MOF-545 we found that lowering the concentration of the modulator BA, while also lowering the total concentration of the solution resulted in MOF particles in the nano regime. Notably, in our hands, other phases of PCN-222/MOF-545-type MOFs seem more accessible compared to NU-1000 analogues, and thus this reaction appears to be more sensitive to modulator concentration.

Using these procedures, we were able to obtain NU-1000 nanocrystals with mean sizes ranging from 75 nm (Fig. 1a) up to 1200 nm (Fig. 1d), and PCN-222/MOF-545 nanocrystals with mean sizes ranging from 350 nm (Fig. 1e) up to 900 nm (Fig. 1h). Other PCN-222/MOF-545 particles with sizes larger than 1000 nm have also been obtained by systematically tuning the reaction conditions (see ESI†). Particle sizes were determined by both scanning electron microscopy (SEM) and dynamic light scattering (DLS) measurements (Fig. S1, ESI†) for NU-1000 materials.

Powder X-ray diffraction (PXRD) patterns of nano-sized NU-1000 and PCN-222/MOF-545 indicate that the MOF particles are one phase and crystalline (Fig. S2 and S3, ESI†). Additionally, thermogravimetric analyses (TGA) of the NU-1000 samples show similar behavior to that reported previously for a microcrystalline version of the material (Fig. S4, ESI†).

Nitrogen sorption isotherms of the activated nano-sized NU-1000 crystallites show a characteristic Type IV sorption profile, with BET surface areas ranging from 2000–2200 m² g⁻¹, which matches

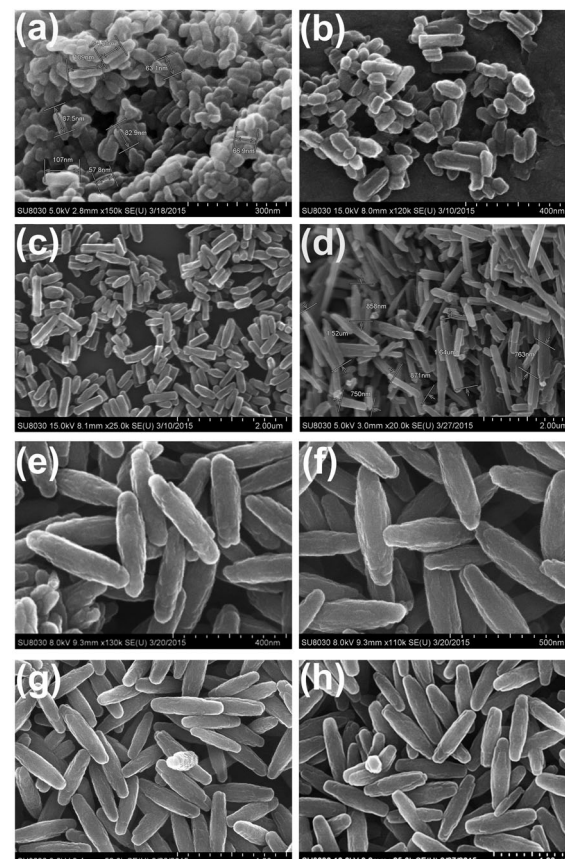


Fig. 1 Scanning electron microscopy (SEM) images of NU-1000 and PCN-222/MOF-545 samples with a range of nano-sized particles. (a) NU-1000 (50–100 nm); (b) NU-1000 (100–200 nm); (c) NU-1000 (300–700 nm); (d) NU-1000 (800–1600 nm); (e) PCN-222/MOF-545 (300–400 nm); (f) PCN-222/MOF-545 (450–500 nm); (g) PCN-222/MOF-545 (600–700 nm); (h) PCN-222/MOF-545 (850–1000 nm).

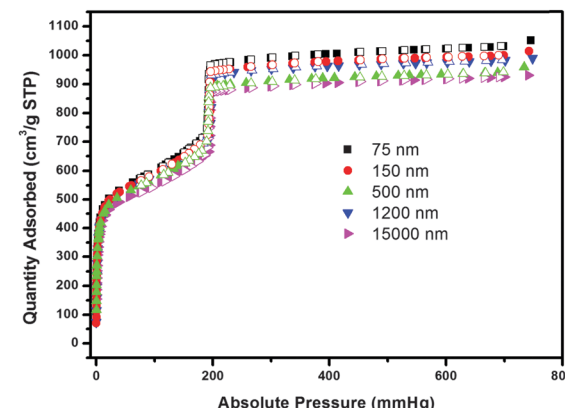


Fig. 2 Nitrogen adsorption (solid) and desorption (open) isotherms at 77 K for NU-1000 samples with different sizes: 75 nm (black), 150 nm (red), 500 nm (green), 1200 nm (blue), and 15 000 nm (pink).

the previously reported surface area for NU-1000 (Fig. 2).^{11a} In addition, density functional theory (DFT) pore size distribution (PSD) calculations indicate that the ratio of mesopores (31 Å) and micropores (10 Å) increases as the size of NU-1000 nanocrystals

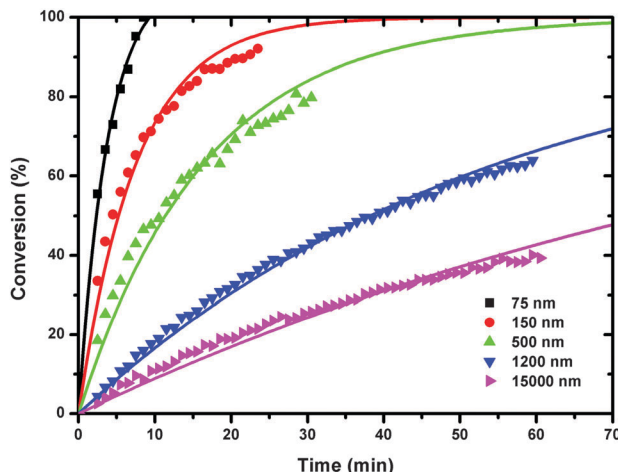


Fig. 3 Rates of hydrolysis of methyl paraoxon using NU-1000 nanocrystals with mean sizes ranging from 75 nm (black), 150 nm (red), 500 nm (green), 1200 nm (blue), to 15 000 nm (pink).

becomes smaller (Fig. S5a, ESI[†]). In the PSD region from 100 Å to 1400 Å, the average pore width of the main peak (corresponding to the space between the crystals) is increasing as the size of NU-1000 particles increases (Fig. S5b, ESI[†]).

We next investigated the rate of hydrolysis of methyl paraoxon as a function of NU-1000 particle size.^{12a,23b,c} As shown in Fig. 3, under fixed reaction conditions (identical catalyst loading, temperature, and reagent concentration), the reaction rate increases inversely with particle size. The half-life ($t_{1/2}$) for the hydrolysis of methyl paraoxon at room temperature dramatically decreases as the particle size decrease (Table S1, ESI[†]). The significantly enhanced reaction rate could be attributed to the larger relative external surface areas of nano-sized NU-1000 particles and/or faster diffusion into nano-sized NU-1000 particles compared to microcrystalline NU-1000.

If we consider NU-1000 as an ideal hexagonal cylinder, the ratio of surface area over volume (S/V) can be denoted as $S/V = 2/h + 2.3/a$, where a is the length of the base edge of the hexagon and h is the length of the cylinder. As the particle sizes decrease, the ratio S/V becomes larger, and accordingly, the rate of hydrolysis increases (Table S2, ESI[†]). This trend of S/V over particle size is further confirmed by a t -plot analysis based on the N_2 isotherms data. The calculated external surface area of the five different-sized NU-1000 materials are $200\text{ m}^2\text{ g}^{-1}$ (75 nm), $150\text{ m}^2\text{ g}^{-1}$ (150 nm), $71\text{ m}^2\text{ g}^{-1}$ (500 nm), $33\text{ m}^2\text{ g}^{-1}$ (1200 nm), $13\text{ m}^2\text{ g}^{-1}$ (15 000 nm), respectively (Table S3, ESI[†]).

In summary, we have reported procedures to effectively control the particle size of NU-1000 (from 75 nm to 1200 nm) and PCN-222/MOF-545 (from 300 nm to 900 nm) in the nano regime by modulating the concentration of modulator and reaction mixture, and/or addition of a secondary monocarboxylic acid modulator. Powder X-ray diffraction patterns and nitrogen sorption experiments indicate that the crystallinity and mesoporosity of NU-1000 is maintained in the nano-sized particles. Additionally, the rate of hydrolysis of methyl paraoxon was investigated using NU-1000 particles with different sizes and determined to increase as the size of the particles decreases.

This observed rate enhancement is attributed to the larger relative external surface areas and/or faster diffusion through the nano-sized MOF crystallites compared to microcrystalline material. We hope that this work will inspire further investigations into the fabrication of nano-sized mesoporous zirconium MOF crystallites for desired applications.

J.T.H. gratefully acknowledges DTRA for financial support (HDTRA1-14-1-0014 for the nano-MOF synthesis and HDTRA1-10-1-0023 for the catalytic study). O.K.F. and S.S.A. contribution to this project was funded by the Deanship of scientific Research (DSR), King Abdulaziz University, Jeddah, under grant no. 23-130-36-HiCi. The authors, therefore, acknowledge with thanks DSR technical and financial support. The authors thank Dr Brian Pate for helpful discussions.

Notes and references

- (a) O. M. Yaghi, M. O'Keeffe, N. W. Ockwig, H. K. Chae, M. Eddaoudi and J. Kim, *Nature*, 2003, **423**, 705–714; (b) G. Ferey, *Chem. Soc. Rev.*, 2008, **37**, 191–214; (c) S. Horike, S. Shimomura and S. Kitagawa, *Nat. Chem.*, 2009, **1**, 695–704; (d) O. K. Farha and J. T. Hupp, *Acc. Chem. Res.*, 2010, **43**, 1166–1175.
- (a) J. A. Mason, M. Veenstra and J. R. Long, *Chem. Sci.*, 2014, **5**, 32–51; (b) L. J. Murray, M. Dinca and J. R. Long, *Chem. Soc. Rev.*, 2009, **38**, 1294–1314.
- 3 J.-R. Li, J. Sculley and H.-C. Zhou, *Chem. Rev.*, 2011, **111**, 869–932.
- 4 L. E. Kreno, K. Leong, O. K. Farha, M. Allendorf, R. P. Van Duyne and J. T. Hupp, *Chem. Rev.*, 2011, **111**, 1105–1125.
- 5 (a) J. Lee, O. K. Farha, J. Roberts, K. A. Scheidt, S. T. Nguyen and J. T. Hupp, *Chem. Soc. Rev.*, 2009, **38**, 1450–1459; (b) J. Liu, L. Chen, H. Cui, J. Zhang, L. Zhang and C.-Y. Su, *Chem. Soc. Rev.*, 2014, **43**, 6011–6061.
- 6 (a) O. K. Farha, A. Ö. Yazaydin, I. Eryazici, C. D. Malliakas, B. G. Hauser, M. G. Kanatzidis, S. T. Nguyen, R. Q. Snurr and J. T. Hupp, *Nat. Chem.*, 2010, **2**, 944–948; (b) O. K. Farha, I. Eryazici, N. C. Jeong, B. G. Hauser, C. E. Wilmer, A. A. Sarjeant, R. Q. Snurr, S. T. Nguyen, A. O. Z. R. Yazaydin and J. T. Hupp, *J. Am. Chem. Soc.*, 2012, **134**, 15016–15021; (c) H. Furukawa, K. E. Cordova, M. O'Keeffe and O. M. Yaghi, *Science*, 2013, **341**, 974.
- 7 (a) K. Schlichte, T. Kratzke and S. Kaskel, *Microporous Mesoporous Mater.*, 2004, **73**, 81–88; (b) M. H. Beyzavi, R. C. Klet, S. Tussupbayev, J. Borycz, N. A. Vermeulen, C. J. Cramer, J. F. Stoddart, J. T. Hupp and O. K. Farha, *J. Am. Chem. Soc.*, 2014, **136**, 15861–15864.
- 8 (a) H. G. T. Nguyen, N. M. Schweitzer, C.-Y. Chang, T. L. Drake, M. C. So, P. C. Stair, O. K. Farha, J. T. Hupp and S. T. Nguyen, *ACS Catal.*, 2014, **4**, 2496–2500; (b) A. M. Shultz, O. K. Farha, J. T. Hupp and S. T. Nguyen, *J. Am. Chem. Soc.*, 2009, **131**, 4204–4205; (c) A. Corma, H. Garcia and F. X. Llabrés i Xamena, *Chem. Rev.*, 2010, **110**, 4606–4655.
- 9 (a) P. W. Siu, Z. J. Brown, O. K. Farha, J. T. Hupp and K. A. Scheidt, *Chem. Commun.*, 2013, **49**, 10920–10922; (b) C. M. McGuirk, M. J. Katz, C. L. Stern, A. A. Sarjeant, J. T. Hupp, O. K. Farha and C. A. Mirkin, *J. Am. Chem. Soc.*, 2015, **137**, 919–925; (c) L. Ma, C. Abney and W. Lin, *Chem. Soc. Rev.*, 2009, **38**, 1248–1256.
- 10 B. Chen, S. Xiang and G. Qian, *Acc. Chem. Res.*, 2010, **43**, 1115–1124.
- 11 (a) J. E. Mondloch, W. Bury, D. Fairén-Jimenez, S. Kwon, E. J. DeMarco, M. H. Weston, A. A. Sarjeant, S. T. Nguyen, P. C. Stair and R. Q. Snurr, *J. Am. Chem. Soc.*, 2013, **135**, 10294–10297; (b) D. Feng, Z.-Y. Gu, J.-R. Li, H.-L. Jiang, Z. Wei and H.-C. Zhou, *Angew. Chem., Int. Ed.*, 2012, **51**, 10307–10310; (c) W. Morris, B. Voloskiy, S. Demir, F. Gándara, P. L. McGrier, H. Furukawa, D. Cascio, J. F. Stoddart and O. M. Yaghi, *Inorg. Chem.*, 2012, **51**, 6443–6445; (d) H. Deng, S. Grunder, K. E. Cordova, C. Valente, H. Furukawa, M. Hmadeh, F. Gándara, A. C. Whalley, Z. Liu, S. Asahina, H. Kazumori, M. O'Keeffe, O. Terasaki, J. F. Stoddart and O. M. Yaghi, *Science*, 2012, **336**, 1018–1023; (e) Z.-Y. Gu, J. Park, A. Raiff, Z. Wei and H.-C. Zhou, *ChemCatChem*, 2014, **6**, 67–75; (f) W. Xuan, C. Zhu, Y. Liu and Y. Cui, *Chem. Soc. Rev.*, 2012, **41**, 1677–1695; (g) L. Song, J. Zhang, L. Sun, F. Xu, F. Li, H. Zhang, X. Si, C. Jiao, Z. Li and S. Liu, *Energy Environ. Sci.*, 2012, **5**, 7508–7520.

- 12 (a) J. E. Mondloch, M. J. Katz, W. C. Isley III, P. Ghosh, P. Liao, W. Bury, G. W. Wagner, M. G. Hall, J. B. DeCoste, G. W. Peterson, R. Q. Snurr, C. J. Cramer, J. T. Hupp and O. K. Farha, *Nat. Mater.*, 2015, **14**, 512–516; (b) L. Ma, J. M. Falkowski, C. Abney and W. Lin, *Nat. Chem.*, 2010, **2**, 838–846.
- 13 (a) X. Liu, Z.-Q. Shen, H.-H. Xiong, Y. Chen, X.-N. Wang, H.-Q. Li, Y.-T. Li, K.-H. Cui and Y.-Q. Tian, *Microporous Mesoporous Mater.*, 2015, **204**, 25–33; (b) A. Schaate, P. Roy, A. Godt, J. Lippke, F. Waltz, M. Wiebcke and P. Behrens, *Chem. – Eur. J.*, 2011, **17**, 6643–6651; (c) A. M. Spokoyny, D. Kim, A. Sumrein and C. A. Mirkin, *Chem. Soc. Rev.*, 2009, **38**, 1218–1227; (d) S. Diring, S. Furukawa, Y. Takashima, T. Tsuruoka and S. Kitagawa, *Chem. Mater.*, 2010, **22**, 4531–4538; (e) J. Cravillon, R. Nayuk, S. Springer, A. Feldhoff, K. Huber and M. Wiebcke, *Chem. Mater.*, 2011, **23**, 2130–2141; (f) L. H. Wee, M. R. Lohe, N. Janssens, S. Kaskel and J. A. Martens, *J. Mater. Chem.*, 2012, **22**, 13742–13746; (g) M. Ma, D. Zacher, X. Zhang, R. A. Fischer and N. Metzler-Nolte, *Cryst. Growth Des.*, 2010, **11**, 185–189; (h) N. A. Khan, I. J. Kang, H. Y. Seok and S. H. Jhung, *Chem. Eng. J.*, 2011, **166**, 1152–1157.
- 14 (a) P. Horcajada, T. Chalati, C. Serre, B. Gillet, C. Sebrie, T. Baati, J. F. Eubank, D. Heurtaux, P. Clayette and C. Kreuz, *Nat. Mater.*, 2010, **9**, 172–178; (b) L.-L. Tan, H. Li, Y.-C. Qiu, D.-X. Chen, X. Wang, R.-Y. Pan, Y. Wang, S. X.-A. Zhang, B. Wang and Y.-W. Yang, *Chem. Sci.*, 2015, **6**, 1640–1644.
- 15 (a) W. Lin, W. J. Rieter and K. M. Taylor, *Angew. Chem., Int. Ed.*, 2009, **48**, 650–658; (b) K. M. Taylor-Pashow, J. Della Rocca, R. C. Huxford and W. Lin, *Chem. Commun.*, 2010, **46**, 5832–5849; (c) J. Della Rocca, D. Liu and W. Lin, *Acc. Chem. Res.*, 2011, **44**, 957–968.
- 16 Y. Wu, J. Han, P. Xue, R. Xu and Y. Kang, *Nanoscale*, 2015, **7**, 1753–1759.
- 17 X. Li, F. Cheng, S. Zhang and J. Chen, *J. Power Sources*, 2006, **160**, 542–547.
- 18 Y. S. Li, F. Y. Liang, H. Bux, A. Feldhoff, W. S. Yang and J. Caro, *Angew. Chem.*, 2010, **122**, 558–561.
- 19 N. A. Khan and S. H. Jhung, *Coord. Chem. Rev.*, 2015, **285**, 11–23.
- 20 W. J. Rieter, K. M. Taylor, H. An, W. Lin and W. Lin, *J. Am. Chem. Soc.*, 2006, **128**, 9024–9025.
- 21 L. G. Qiu, T. Xu, Z. Q. Li, W. Wang, Y. Wu, X. Jiang, X. Y. Tian and L. D. Zhang, *Angew. Chem., Int. Ed.*, 2008, **47**, 9487–9491.
- 22 (a) J. E. Mondloch, M. J. Katz, N. Planas, D. Semrouni, L. Gagliardi, J. T. Hupp and O. K. Farha, *Chem. Commun.*, 2014, **50**, 8944–8946; (b) T.-F. Liu, D. Feng, Y.-P. Chen, L. Zou, M. Bosch, S. Yuan, Z. Wei, S. Fordham, K. Wang and H.-C. Zhou, *J. Am. Chem. Soc.*, 2015, **137**, 413–419; (c) D. Feng, K. Wang, J. Su, T. F. Liu, J. Park, Z. Wei, M. Bosch, A. Yakovenko, X. Zou and H. C. Zhou, *Angew. Chem., Int. Ed.*, 2015, **54**, 149–154; (d) S. B. Kalidindi, S. Nayak, M. E. Briggs, S. Jansat, A. P. Katsoulidis, G. J. Miller, J. E. Warren, D. Antypov, F. Corà, B. Slater, M. R. Prestly, C. Martí-Gastaldo and M. J. Rosseinsky, *Angew. Chem., Int. Ed.*, 2015, **54**, 221–226.
- 23 (a) J. E. Mondloch, M. J. Katz, W. C. Isley III, P. Ghosh, P. Liao, W. Bury, G. W. Wagner, M. G. Hall, J. B. DeCoste and G. W. Peterson, *Nat. Mater.*, 2015, DOI: 10.1038/nmat4238; (b) M. J. Katz, J. E. Mondloch, R. K. Totten, J. K. Park, S. T. Nguyen, O. K. Farha and J. T. Hupp, *Angew. Chem., Int. Ed.*, 2014, **53**, 497–501; (c) M. J. Katz, S.-Y. Moon, J. E. Mondloch, M. H. Beyzavi, C. J. Stephenson, J. T. Hupp and O. K. Farha, *Chem. Sci.*, 2015, **6**, 2286–2291.
- 24 D. A. Gomez-Gualdrón, O. V. Gutov, V. Krungleviciute, B. Borah, J. E. Mondloch, J. T. Hupp, T. Yildirim, O. K. Farha and R. Q. Snurr, *Chem. Mater.*, 2014, **26**, 5632–5639.
- 25 C.-W. Kung, T. C. Wang, J. E. Mondloch, D. Fairen-Jimenez, D. M. Gardner, W. Bury, J. M. Klingsporn, J. C. Barnes, R. Van Duyne, J. F. Stoddart, M. R. Wasielewski, O. K. Farha and J. T. Hupp, *Chem. Mater.*, 2013, **25**, 5012–5017.
- 26 D. Feng, H.-L. Jiang, Y.-P. Chen, Z.-Y. Gu, Z. Wei and H.-C. Zhou, *Inorg. Chem.*, 2013, **52**, 12661–12667.
- 27 D. Feng, Z.-Y. Gu, Y.-P. Chen, J. Park, Z. Wei, Y. Sun, M. Bosch, S. Yuan and H.-C. Zhou, *J. Am. Chem. Soc.*, 2014, **136**, 17714–17717.